Capabilities of micro-Raman spectrometry for the identification of uranium ore concentrates from analysis of single particles

Fabien Pointurier, Doris Ho Mer Lin, Dario Manara, Olivier Marie, Thomas Fanghänel, Klaus Mayer

Capabilities of micro-Raman spectrometry for the identification of uranium ore concentrates from analysis of single particles

Fabien Pointurier[1*], Doris Ho Mer Lin[2,3], Dario Manara[2], Olivier Marie[1], Thomas Fanghänel[2,4], Klaus Mayer[2]

[1] *CEA, DAM, DIF, F-91297 Arpajon, France*

[2] *European Commission, Joint Research Centre - Karlsruhe (JRC-K), P.O. Box 23 40, 76125 Karlsruhe, Germany*

[3] *DSO National Laboratories, 12 Science Park Drive, Singapore 118225*

[4] *Ruprecht-Karls-Universität Heidelberg, Physikalisch-Chemisches Institut, Im Neuenheimer Feld, Germany*

Abstract

It has been proven, by the analysis of macroscopic amount of materiel pressed into pellets, that Raman spectrometry is a well suited technique to determine precisely the chemical compositions of uranium ore concentrates (UOCs), which is useful information for nuclear forensics and safeguards. However, as in some cases, only low amounts of UOC are available or the sample is a mixture of different UOCs, there is a need to carry out the identification at the individual grain or particle's level. To evaluate the capability of micro-Raman spectrometry (MRS) for this purpose, 15-30 particles with typical sizes of a few micrometers from five UOCs of known bulk chemical compositions (uranyl peroxide – UP, sodium di-uranate – SDU, ammonium di-uranate – ADU, tri-uranium octo-oxide – TUO, and uranyl hydroxide – UH), production process and origins, were analyzed. Spectra were also compared with the ones obtained with macroscopic amounts of material pressed into pellets. Results show that for some UOCs (SDU, ADU, UH), micro-Raman spectra are reproducible from one particle to another and in good agreement on one side with available bibliographic data and on the other side with Raman spectra performed on macroscopic amounts of UOC. However, spectra of particles from the UP and TUO UOCs show that these compounds are mixtures of three species which were

* Corresponding author. E-mail : fabien.pointurier@cea.fr, phone : +33 1 69 26 49 17.

identified. In these cases, an acceptable agreement is obtained between the average Raman spectrum on compressed pellets and the one of most abundant species in analyzed particles. Consequently, an UOC compound or components of a mixture of UOCs can be reliably identified by the analyses of a limited number of isolated particles of a few µm in size by means of MRS.

Keywords: Nuclear forensics; Raman spectroscopy; Uranium ore concentrates; Particle analysis; Bulk analysis.

1. Introduction

Nuclear forensics or nuclear forensic science is a relatively young discipline, evolved from the need to tackle illicit trafficking of nuclear material. The multi-disciplinary field of nuclear forensics serves to answer several important questions such as “what is the material?”, “where did it come from?”, “who does it belong to?” and “how did it get out of control?” Determining the nature of the material, its potential use and industrial history, as well as attributing its origin are drawn from several measurable parameters, also known as *signatures* or *fingerprints*. They can be derived by the inheritance from the source material itself or by industrial processes. These parameters therefore include the analysis of major and minor constituents, morphology and age of the material [1—3].

Uranium ore concentrates (UOCs), also colloquially known as yellow cakes, are the major input material for the nuclear industry and are traded in large quantities. Therefore, detection and identification of UOCs are of great interest for both nuclear safeguards and forensics. Moreover, to our knowledge, three independent nuclear forensic investigations have been reported on this class of material during the last decades [4—6]. Following the extraction of uranium, the ore is further milled and purified, concentrated and precipitated to obtain the ore concentrate. Several precipitating reagents can be used such as ammonium carbonate, ammonia/ammonium hydroxide, magnesia, sodium hydroxide and hydrogen peroxide. Therefore, these reagents and the associated processes give rise to the different compositions of UOCs: ammonium uranyl-carbonate (AUC), ammonium di-uranate (ADU), uranyl hydroxide (UH), sodium di-uranate (SDU) and uranyl peroxide (UP), respectively. These compounds can be also calcined to obtain tri-uranium octa-oxide (U_3O_8 or TUO). So, the chemical composition of the UOCs is a useful fingerprint for identifying the origin and purification of an UOC material. As a consequence, it is important to develop the corresponding analytical methodologies for measuring these signatures.

It has been demonstrated recently that Raman Spectrometry (RS) is a useful tool for the identification of uranium species for nuclear forensics [7—12] and nuclear safeguards [13—18, 40].

Regarding nuclear forensics, process-related impurities in UOCs were also detected by RS in bulk material [7—10]. Different Raman spectrometers, ranging from small-scale (such as hand-held) model to bench-top and laboratory models, were evaluated and compared [8]. Most of the time, material analyzed in the frame of a nuclear forensic investigation is available in relatively large amounts (> mg), although application of methodologies normally relevant for nuclear forensics, like the use of SIMS to determine the isotopic ratios of oxygen [19] or uranium [20] were applied to individual particles. However, local micro–analysis capability is potentially interesting in three cases:

a. Micrometric particles are identified in the inner or outer surfaces of the container and/or packaging of the bulk seized nuclear material. These particles may be of the same composition as the bulk nuclear material (contamination), but can also be of different compositions and so may add additional information about origin of the bulk nuclear material.
b. The seized sample is a mixture of several compounds. In such a case, a bulk analysis provides only averaged information. Micro–analysis at the scale of the single particle is therefore necessary to identify each individual components of the mixture and to increase probabilities to identify the origin of the whole sample or of its components. In the case of UOCs, it is well-known that different purification processes can be carried out to transform U-ore into UOC, leading to different UOC compounds. Moreover, it is a common practice in nuclear industry to mix UOCs of different origins, with different impurity levels, before further proceeding to the first steps of the conversion step.
c. The seized sample itself is a very small one, and contains only minute amounts of material. This small amount of material may have to be divided into several sub–samples for different kinds of analysis, possibly carried out by different laboratories (among them, destructive analytical techniques like mass spectrometry). Therefore, quantity of material in sub–samples available for analysis by RS may be extremely low (µg or below).

So, there is obviously a need for a capability to perform analysis on microscopic amounts of materials, typically on particles whose size do not exceed a few µm. Analyses by Micro-Raman Spectrometry (MRS) of micrometer-size particles made of various uranium oxides (UO_2, UO_3, U_3O_8, $UO_4{\cdot}4(H_2O)$) [15, 16, 18, 21], uranyl fluoride (UO_2F_2) [14, 22], and UF_4 [23] had already been described. These compounds were successfully identified and spectra are in acceptable agreement with the one reported previously from macroscopic amounts of the same materials. However, the question that unavoidably arises from these measurements is to know if analysis of micrometric particles is representative of the “bulk” material, i.e. if the material is homogeneous at the micrometer scale. Inversely, it can be highly valuable, if need be, to identify individual components of a mixture of several UOCs from different origin, which is obviously not possible when analysis is

performed on a larger scale. To our knowledge, analysis of several UOCs of known chemical compositions by MRS at the particle's level has never been reported, and, to our knowledge, the degree of homogeneity of the Raman vibrational spectrum of these materials at the micrometer scale is not known.

In this study, samples of industrial UOCs from five different chemical compositions are analyzed using MRS both on macroscopic ("bulk") amounts of materials compressed into pellets and on individual particles extracted from the bulk samples. Objectives of this study are: i) by comparing with bibliographic data and spectra obtained from Raman analysis on pressed pellets, to determine if the corresponding UOC can or cannot be reliably identified; ii) to evaluate homogeneity of the UOCs at the particle's scale; iii) in case of heterogeneous UOC (i.e. mixture of different UOCs), to identify components of the mixture.

It should be noted that, to our knowledge, the use of MRS for analysis of isolated individual particles coming from industrial UOCs is reported for the first time. Besides, as far as we know, no data exist about homogeneity of the Raman spectra of UOCs at the micrometer-size scale.

2. Experimental

2.1. Industrial UOCs for bulk Raman analysis

Five industrial UOCs, certainly the most commonly found compositions of UOCs, were investigated in this study: uranyl peroxide – UP, sodium di-uranate – SDU, ammonium di-uranate – ADU, tri-uranium octo-oxide – TUO, and uranyl hydroxide – UH. Table 1 provides an overview of the information associated with each sample. The information includes the location where the sample was produced, the type and nature of uranium-ore that was mined and the chemical processes involved in producing the UOCs. A picture of the different compounds is given in Fig. S1. The samples are in powder form and were pressed into pellet using a hydraulic press (SPEX Industries Inc., USA) to facilitate handling and to minimize possible contamination. A pressure of approximately 74 MPa was applied. These samples reflect five commonly found compositions of UOCs. In previous studies, it has been demonstrated that RS analysis on material pressed into pellets allows distinguishing each compound one from another [7, 9].

Table 1

2.2. Deposition on carbon disks for Raman analysis on individual particles

Raman SPA analyses were carried out on particles deposited on 1-inch diameter carbon disks. Two methods were used for particle depositions onto carbon disks.

The samples from El Mesquite (UP) and Susquehanna (UH) UOCs were prepared at the European Research Center – Karlsruhe (JRC-K) in the following way. Firstly, a 1-inch carbon disk with a 1.3 cm double-sided adhesive tape in the middle was placed in a vacuum impactor. Next, a very small amount of sample in powder form was spread on a piece of clean filter paper. The vacuum impactor was then connected to a pump at very low flow rate (~0.5 $l \cdot min^{-1}$) and was wiped briefly across the filter paper containing the sample. The disk was then removed from the impactor and sent to CEA for analysis. Fig. S2 (left) shows an example of a well-dispersed deposition from the Susquehanna UOC.

The samples from Denison (ADU, Ranstad (SDU) and Olympic Dam (TUO) UOCs were prepared at the Commissariat à l'Energie Atomique et aux energies alternatives (CEA) center in Arpajon (France), where only limited amounts of uranium can be handled. Depositions were carried out in the following way: inside a glove bag, a very small amount of bulk UOC (in the µg to the mg range) was transferred into a glass vial filled with a few ml of pure ethanol. After gently shaking the vial, 100 µl of ethanol containing uranium particles were sampled and deposited onto a glassy carbon disk. Ethanol was evaporated at room temperature. Fig S2 (right) shows the deposition of the Denison UOC. As a consequence of the very low amount of material sampled, particles are less abundant and on average smaller in depositions prepared at CEA, than the ones in depositions prepared at JRC-K. However, enough particles with sufficient sizes (>2 µm) can be easily found and analyzed.

2.3. MRS used for Raman bulk analysis

'Senterra' bench-top model of Raman spectrometer from Bruker (Germany) was used for the bulk analysis (BA) of the UOCs. Measurement using silicon standard was carried out daily prior to measurements to ensure that the sensitivity of the instrument is kept constant on the different days of measurement. Calibration of wavenumbers is performed automatically by the instrument.

Two different laser wavelengths, 785 and 532 nm, are available with the 'Senterra' RS. The former permits largely the measurements of all samples, while the latter is not favorable as the high energy causes much fluorescence and sample degradation due to the heat induced from the laser (photolysis). Therefore, laser power of 10 mW of the 785 nm laser is used on the samples. Integration times are 10 s for all samples with exception of TUO Olympic Dam (25 s). The selected

spectral range is 90-1560 cm^{-1} as no peaks are observed outside this region. A minimum of five spectra were taken for each sample at different spots or areas.

'Opus' software from Bruker was used to process the spectra. Spectra were cut at low wavenumbers to remove the spikes which would otherwise affect the baseline correction. The wavenumber at which spectra were cut varies from sample to sample and occasionally can differ for different spectra from the same sample, depending on the background noise. Each spectrum is then corrected for its fluorescence background. The rubber-band concave scattering was applied universally to all spectra with 64 baseline points and 5 iterations. Lastly, overlapping peaks for each spectrum were de-convoluted by curve fitting. Initial peak shape for all selected peaks was based on a combination of Lorentzian and Gaussian and curve fitting carried out using Levenberg-Marquardt method. The step was reiterated until there was no further improvement to the value of Residual RMS error.

2.4. MRS used for individual single particle analysis

Another bench-top Raman model, 'InVia' from Renishaw (Wotton-Under-Edge, Gloucestershire, UK) was used for the single particle analysis (SPA) of the same UOCs. Calibration of the spectrometer was carried out using silicon wafer with the 520.5 cm^{-1} band. The 'InVia' is also equipped with two laser wavelengths, 785 nm and 514 nm with maximum power of 200 and 50 mW respectively. In this study, the same laser frequency at 785 nm is also used for 'InVia'. 'Wire' software from Renishaw was used to process the spectra. The spectra obtained from the 'InVia' Raman spectrometer were processed in the following manner. Firstly, baseline of each spectrum was individually corrected by manually selecting points across the baseline and using cubic spline interpolation. Subsequently, each spectrum was subjected to a curve fitting procedure. Curves are initially added by the user (curve fit model) at the approximate centers and heights of the bands. Widths are set at default values but can be adjusted manually. The user has to define the number of bands in a region of interest. An algorithm performs automatically much iteration until the best fit is achieved, by minimizing the sum of the squared deviations of the curve fit model to the data. Bands can be added or removed afterwards to obtain a better fit.

Main characteristics of the two Raman spectrometers are gathered in Table S1. One of the main differences between the two instruments is the smaller analyzed area of the 'InVia' (~4 μm^2 with the 785 nm laser and the 100× objective) with respect to the 'Senterra' (~20 μm^2 with the 785 nm laser and the 20× objective).

3. Results and discussion

3.1. General comments

5–10 and 15–30 measurements were carried out on UOC pellets (BA) and on individual UOC particles (SPA), respectively. Sizes of the micro-objects analyzed by SPA (referred in the following to as 'particles') vary from ~2 µm to a few tens of µm. It should be noted that laser power for SPA is limited for all UOCs to 0.1% of the laser full power (~0.3 mW) for all particles. Higher power causes sample degradation due to the heat induced by the laser (observed spectra is the one of TUO). BA spectra obtained for larger analyzed areas (ca. 20 μm^2) and on compressed materials are quite well reproducible as only one type of spectrum is identified for each UOC and it is always characterized by the same major peaks at the same wavenumbers within a few cm^{-1}.

Spectral were acquired in the range 200—1200 cm^{-1}. It is well known that most of the bands related to uranium oxide compounds can be found below 900 cm^{-1} [24—40]. In particular, the frequencies caused by the O-U-O symmetric stretching are reported in the 700—900 cm^{-1} region. In other respects, specific bands from molecular impurities like sulfates, carbonates, chlorates, nitrates, etc., are reported between 900 and 1200 cm^{-1} [41—44].

In the following, average spectra obtained by SPA for each of the studied UOCs are systematically compared with the average spectrum obtained for the same compound by BA. When different types of SPA spectrum are observed for a given UOC, the average spectrum of each type is provided. It should be mentioned that, as Raman intensities may vary significantly from one particle to another (up to a factor of ten within the same analytical conditions), averaging is carried out on normalized SPA spectra with respect to the height of the most intense peak in the region of interest. Results are discussed separately for each UOC. In some cases, Raman bands are very close and must be de-convoluted by means of the fitting algorithms available in the Raman spectrometers, which may produce a mathematical approximation in the position of the peak centers. Lastly, detection and assignment of Raman bands in the impurity region will be discussed separately. Uncertainties associated to the band positions are standard deviations on the band positions measured for all spectra.

3.2. Results for El Mesquite UOC (UP)

25 individual particles, with sizes ranging from ~3 to ~40 µm, were analyzed by SPA. Whereas all BA spectra were similar, Raman SPA produced three distinct types of spectra (Fig. 1). The most prevalent one, referred to as P1 (17 particles out of 25), is characterized by two major bands at 830±1 and

868±1 cm^{-1} and is very similar to the BA average spectrum, for which major bands are at 831±1 and 868±1 cm^{-1}**.** These bands match very well the ones regarded as characteristic of U peroxide (more precisely 'studtite' ($UO_4{\cdot}4(H_2O)$) or 'meta-studtite' ($UO_4{\cdot}2(H_2O)$) depending on the hydration level of the molecule), which is the expected compound, according to several authors [13, 15, 27, 29, 31, 37]. Wavenumbers of the less intense bands detected by both BA and SPA for P1 particles are also in good agreement (low intensity bands at ~280 cm^{-1}, ~355 cm^{-1}, and ~550 cm^{-1}) and are relatively close to the bands reported by Bastians *et al*. [29] for heated studtite or meta-studtite.

Five particles out of 25 show another type of spectrum referred to as P2, with a single major band at 939±2 cm^{-1} with a shoulder at 824±3 cm^{-1} in the 700—900 cm^{-1} region. This is in very good agreement with the band reported between 830 and 845 cm^{-1} by various authors for hydrated UO_3 compounds: 'schoepite' [27, 37, 45] or 'meta-shoepite' [46]. Most of the low intensity bands observed in the BA spectra are also observed in the P2 spectra at 252±3 cm^{-1}, 354±2 $cm^{-1}$and 549 cm^{-1}. Lastly, three particles out of 25, referred to as P3, show a slightly different spectrum with a broad band at 750±3 cm^{-1} and a high intensity band at 813±3 cm^{-1}. This spectrum is very close to the one reported by Mellini & Riccobono [31] for the compound formed at the surface of oxidized uranium metal disposed in the environment and regarded by the authors as schoepite.

So Raman SPA shows that El Mesquite UOC, which is expected to be UP (i.e. $UO_4{\cdot}4(H_2O)$), is not homogeneous at the micrometric scale and is in fact composed of three different chemical compounds, whereas Raman BA allows detecting only the most abundant compound (UP, P1-type of particles). This is consistent with the results from Plaue [39] who demonstrated by means of XRD analysis that this UOC contains $UO_3.2H_2O$ (schoepite) as well as $UO_4{\cdot}4(H_2O)$ (studtite) and $UO_4{\cdot}2(H_2O)$ (meta-studtite).

Figure 1

3.3. Results for Ranstad UOC (SDU)

20 individual particles, with sizes ranging from ~3 to ~20 µm, were analyzed. Raman SPA spectra are perfectly reproducible and are in excellent agreement with the ones evidenced by Raman BA (Fig. 2).

Besides, both BA and SPA Raman spectra are in good agreement with the one reported by Volkovich *et al*. [47] for sodium di-uranate, i.e. main bands at 233 (m), 274 (m), 420 (s), 584 (m), 752 (m), 779 (s), 788 (vs, i.e. the most intense peak of the spectra), and 826 (m) cm^{-1}. It can be concluded from that the Ranstad UOC is chemically homogeneous at the micrometric scale.

Figure 2

3.4. Results for Denison UOC (ADU)

20 individual particles, with sizes ranging from ~2 to ~10 µm, were analyzed. Raman SPA spectra are well reproducible and are globally in agreement with the ones evidenced by Raman BA (Fig. 3), with the notable exception of a slight shift of the major band of the spectra, assigned to uranyl symmetric stretching, on average at 830±1 cm^{-1} for SPA and at 825±1 cm^{-1} for BA.

However, Raman BA and SPA spectra are globally in good agreement with the ones reported by D.M.L. Ho *et al.* for different ADUs [7—10]. It should be noted that the exact position of uranyl symmetric stretching band reported in these studies vary between 816 and 826 cm^{-1}. Actually, the compound called ADU has been produced in different ways and it showed a variety of compositions and crystal structures [48, 49]. The most common stoichiometric composition for ADU is $(NH_4)_2 \cdot U_2O_7$. However, there are still some debates over its exact composition and structure [48, 49]. Besides, the formation of ammonium uranium oxide hydrate ($NH_3 \cdot 2UO_3 \cdot H_2O$) as an intermediate by moderate heating in the temperature region 145-220°C along with amorphous UO_3 was reported by Raje *et al.* [50]. So as a possible explanation for the shift between the most intense bands of SPA and BA, we assume that higher power density in the case of BA with respect to BA (~0.3 mW over ~4 μm^2 i.e. ~0.075 $mW \cdot \mu m^{-2}$ for SPA, ~10 mW over ~20 μm^2 i.e. ~0.5 $mW \cdot \mu m^{-2}$ for BA) may lead to some changes in the chemical phase of the material. Besides, compression into pellets carried out for Raman BA may also produce a slight compositional change of ADU through moderate heating. This should be confirmed by further experiments, for instance by gradual increase of laser power and observation of possible changes in the Raman spectra, especially for the position of the uranyl symmetric stretching band.

Figure 3

3.5. Results for Olympic Dam UOC (TUO)

Special attention was paid to this compound obtained after calcination of a primary UOC. It is of uttermost importance to determine if the primary UOC can be tracking down through analysis of

individual particles by MRS. Besides, depending on the temperature of calcination of the primary UOC, different compositions are obtained. Manna et al. [48] reported that calcination of ADU at 450°C, 550°C and 650°C produces a mixture of monoclinic β-UO_3 and orthorhombic α-U_3O_8 (termed as 'uranium oxide'). However, uranium oxide produced at 750°C is a single phase compound of orthorhombic α-U_3O_8, whereas calcination above 900°C leads to an hypo-stoichiometric compound U_3O_{8-x}, possibly U_8O_{21} [48]. According to Eloirdi and co-workers [49], calcination of ADU at 600°C leads to unstable U_3O_8 which evolves into to β-UO_3 after cooling. So TUO Raman SPA spectra may be heterogeneous either because presence of residual primary UOC(s) or because of incomplete calcination into U_3O_8.

30 individual particles, with sizes ranging from ~2 to ~15 µm, were successfully analyzed. Whereas all BA spectra are perfectly reproducible, SPA produced three distinct types of spectra (Fig. 4). The most prevalent one, referred to as P1 (16 particles out of 30), is very similar to the one obtained by Raman BA on a pellet of Olympic Dam UOC. These spectra are characterized by an intense band at ~410 cm^{-1}, two shoulders (medium) at ~340 and ~480 cm^{-1}, medium bands at ~250 and ~800 cm^{-1} and a weak broad band at ~750 cm^{-1}. These spectra are consistent with the ones reported by several authors for U_3O_8 [15, 21, 24, 26, 30, 35, 36], although weak bands at ~840 and ~865 cm^{-1} are also observed in the BA spectra, and at ~820 cm^{-1} in the P1-SPA Raman spectra. By contrast, P2 and P3 spectra (obtained for 10 and 4 particles, respectively) are quite similar to the P1 and BA ones in the 200—800 cm^{-1} region but are characterized by intense bands at ~860 cm^{-1} and at ~840 cm^{-1}, respectively. Assignment of these peaks is unclear, although the second one may correspond to hydrated UO_3 ($UO_3 \cdot 2(H_2O)$ or 'shoepite') akin to uranyl hydroxide ($UO_2 \cdot (OH)_2$). Our interpretations of these observations are the following: i) BA spectra are a "weighed average" of P1, P2, and P3 SPA spectra; so Raman SPA allows distinguishing more clearly different chemical phases in the UOC whereas BA Raman shows only an "average spectrum" of the different phases; ii) chemical phases which correspond to P2 and P3 spectra may be primary UOCs which remain in the U oxide because of incomplete calcination, or altered phases of incompletely calcined U_3O_8, especially in the case of single particles, more vulnerable to oxidization or hydration than bulk material.

Figure 4

3.6. Results for Susquehanna UOC (UH)

15 individual particles, with sizes ranging from ~5 to ~20 µm, were analyzed. Spectra are well reproducible and in very good agreement with the ones obtained by Raman BA (Fig. 5). Both average BA and SPA spectra are characterized by a very strong band at ~840 cm^{-1} (841±2 cm^{-1} for SPA and 839±1 cm^{-1} for BA), a shoulder at 832 cm^{-1}, two medium broad bands at ~750 and ~690 cm^{-1}, and several weak bands in the 200—600 cm^{-1} region.

Besides, our spectra are in good agreement with the ones reported in other publications for uranyl hydroxide [7] or for 'schoepite' (hydrated UO_3 whose composition is akin to one of UH) [27, 33, 37, 40, 45, 46].

Figure 5

3.7. Detection of molecular impurities

Several bands were observed for all studied UOCs in the 900-1200 cm^{-1} region (fig. 6) with exception of El Mesquite UOC. However, most of these bands were of very low intensities and were not observed for all particles. This lack of reproducibility suggests that the corresponding impurities are not homogeneously distributed between particles. Moreover, identification of specific molecular species is difficult and assignments of these bands may be ambiguous given the closeness of band positions of many species and lack of Raman reference for other chemical compounds which could be present in the materials. In spite of this, we make below an attempt to rely some of the Raman bands in the impurity region with chemical species which may be present in the studied UOCs knowing the reagents used in their purification processes.

Figure 6

Ranstad UOC: the most intense band in the impurity region at 1075±1 cm^{-1} may be assigned to Na_2CO_3, a compound used for stripping U and whose Raman spectrum is mainly characterized by a band at 1078 cm^{-1} [7, 43] or 1081 cm^{-1} [44].

Denison UOC: several weak peaks were also detected in the impurity region for most of the analyzed particles, at 986±3 (shoulder), 1001±1, 1012±1, 1048±2, and 1062±2 cm^{-1}. The band at 1012 cm^{-1} could be assigned to $CaSO_4$ (major band at 1009 cm^{-1} for hydrated compound and 1015 cm^{-1} for anhydrous compound [7, 43]) which is not unlikely as H_2SO_4 is used in the extraction process by in

situ leaching and as CaO along with NH_3 is used for impurity precipitation. In the same way, the band at 1048 could be assigned to HNO_3 (1047 cm^{-1} [7]) or more probably to $(NH_4)_2{\cdot}NO_3$ (1043 cm^{-1} [7], 1038 cm^{-1} [43]), and the band at 1062 cm^{-1} could be assigned to $NaNO_3$ (1067 cm^{-1} [7], 1069 cm^{-1} [43]), respectively. However, this may confirm observations made by Raje and co-workers [50] by means of FTIR suggest the presence in ADU of $NH_4{\cdot}NO_3$ as an impurity, entrapped in the ADU matrix during its synthesis.

Olympic Dam UOC: one weak band and two very weak and broad bands were detected in the impurity region at 1015±3, 1070±2 and 1097±3 cm^{-1}, respectively, for most of the analyzed particles. Only the first band could be reliably assigned to $CaSO_4$ [7, 43].

Susquehanna UOC: in the impurity region, one weak band was detected at 1014±3 cm^{-1} for most of the particles and two very weak bands were observed at 1045±1 and 1095±3 cm^{-1} for a few particles. Again, the first band could be reliably assigned to $CaSO_4$ [7, 43] whereas the very weak band at 1045 cm^{-1} could be the signature of $NH_4{\cdot}NO_3$ or residue of HNO_3.

This attempt of assignment of the weak bands observed in the impurity region shows clearly that more work should be done on this topic, for instance by longer acquisition time in the impurity region, by analysis of particles of the pure compounds expected to be present as impurity in the UOC particles so as to define more precisely the band positions, or possibly by correlating the information derived from the Raman spectrum with the detection of elemental impurities by EDX in the same particle thanks to a coupling device between a SEM (equipped with an EDX analyzer) and the MRS ("SEM-SCA", Renishaw).

4. Conclusions

In this study, five different UOCs, corresponding to the most frequently encountered UOCs, of expected chemical compositions UP, SDU, ADU, TUO, and UH, and known production processes and origins, were investigated by micro-Raman spectroscopy. Analyses were carried out on one hand on macroscopic amounts of material (Raman bulk analysis: BA) compressed into pellets with a 20x objective (spot area ~20 μm^2) and on the other hand on single isolated particles (diameters 2—30 µm, Raman Single Particle Analysis: SPA) with a 100x objective (spot area ~4 μm^2). The Raman spectra obtained for the bulk samples and the corresponding particle measurement were systematically compared.

In details, for Ranstad (SDU), Denison (ADU), and Susquehanna (UH) UOCs, Raman SPA produces a unique and well reproducible spectrum, similar to the one obtained by Raman BA. However, in the

case of El Mesquite (UP) and Olympic Dam (TUO) UOCs, SPA gives three types of spectrum whereas a single spectrum is obtained by BA. Interestingly, the majority SPA spectrum, obtained for most of the particles, is fairly consistent with the BA spectrum. In the case of El Mesquite UOC, detection of UP and hydrated UO_3 (schoepite) is consistent with results of analysis by means of XRD reported elsewhere [39].

Overall, results of BA and SPA are in good agreement, which demonstrates that identification of the main UOC compounds can be achieved unambiguously from a few particles with sizes of a few µm. It has already been demonstrated previously [7—10] that MRS allows identifying the various types of UOCs starting from macroscopic amounts of material compressed into pellets. This study demonstrates that the same conclusion can be drawn if only sparse particles of a few µm in diameter are available for analysis by MRS. Moreover, another important conclusion is that Raman SPA also allows identifying the individual components of a mixture of several UOCs, which is very useful as it is a common practice in the nuclear industry to mix UOCs. These capabilities are obviously of great interest for nuclear forensics but also for nuclear safeguards, especially in the case of 'environmental sampling' which consists in collecting trace amounts of nuclear materials, in the form of particulate matter, by wiping surfaces in inspected facilities with cotton substrates.

Further studies need to compare Raman spectra obtained with UOCs of the expected same chemical composition but which originate from different production plants. Another perspective is a more thorough exploitation of the Raman bands in the impurity region (900-1200 cm^{-1}) possibly related to molecular impurities coming from reagents used for the extraction – purification – concentration process. Systematic XRD analysis could also be performed on each compound to confirm or not presence of several phases is some UOCs. Lastly, another promising path of research is to implement a combined SEM/EDX – MRS coupling device to obtain for the same particle the Raman spectrum, the elemental composition (by means of EDX spectroscopy) and SEM images. This would allow establishing correlations between chemical compounds (main UOC phases, molecular impurities) and information related to the industrial process (elemental impurities, size and micro-structure of particles).

Acknowledgement

The authors wish to acknowledge the UK Support Program to the IAEA, Nexia Solutions (Springfield, UK) and IAEA for providing samples of yellow cakes. The support provided by the Australian Safeguards and Non-proliferation Office (ASNO) for the acquisition of samples from Australia is highly

appreciated. The authors will like to thank the Institute for Nuclear Waste Disposal, Karlsruhe (INE), Germany, for the use of Bruker Senterra. Colleagues from ITU (A. Nicholl, M. Hedberg, M. C. Vincent and N. Albert) and INE (D. Schild and P. Lindqvist-Reis) are acknowledged for their kind support.

References

[1] K. Mayer, M. Wallenius, Z. Varga, Chem. Rev. 113 (2012) 884-900.

[2] K. Mayer, M. Wallenius, I. Ray, Analyst 130 (2005) 433-441.

[3] K. Mayer, M. Wallenius, T. Fanghänel, J. Alloys Compounds 444-445 (2007) 50-56.

[4] E. Keegan, M.J. Kristo, M. Colella, M. Robel, R. Williams, R. Lindvall, G. Eppich, S. Roberts, L. Borg, A. Gaffney, J. Plaue, H. Wong, J. Davis, E. Loi, M. Reinhard, I. Hutcheon, Forensic Science International 240 (2014) 111-121.

[5] Z. Varga, Proc. Radiochim. Acta 1 (2011) 1-4.

[6] P.A. Budinger, T.L. Drenski, A.W. Varnes, J.R. Mooney, Anal. Chem. 52 (1980) 942A-948A.

[7] D. Ho Mer Lin, D. Manara, Z. Varga, A. Berlizov, T. Fanghänel, K. Mayer, Radiochim. Acta 101 (2013) 779-784.

[8] D. Ho Mer Lin, D. Manara, P. Lindqvist-Reis, T. Fanghänel, K. Mayer, Vib. Spectros. 73 (2014) 102-110.

[9] D.M.L. Ho, A.E. Jones, J.Y. Goulermas, P. Turner, Z. Varga, L. Fongaro, T. Fanghänel, K. Mayer, Forensic Sci. Intern. 251 (2015) 61-68.

[10] A. Berlizov, D.M.L. Ho, A. Nicholl, T. Fanghänel, K. Mayer, J. Radional. Nucl. Chem. (2016) 285-295.

[11] F. Pointurier, O. Marie, Proc. International Conference on Advances in Nuclear Forensics, IAEA-CN-218/80, Vienna, Austria, 7-10 July 2014.

[12] S. Holmgren-Rondahl, F. Pointurier, et al., J. Radioanal. Nucl. Chem. 315 (2018) 395-408.

[13] A. J. Pidduck, M. R. Houlton, G. M. Williams, D. L. Donohue, IAEA-CN-148/115, Proc. Symp. on Intern. Safeguards, Vienna, Austria, 16–20 October 2008, 781-789.

[14] R. Kips, A.J. Pidduck, M.R. Houlton, et al., Spectrochim. Acta B 64 (2009) 199-207.

[15] F. Pointurier, O. Marie, Spectrochim. Acta Part B 65 (2010) 797-804.

[16] F. Pointurier, O. Marie, J. Raman Spectrosc. 44 (2013) 1753-1759.

[17] E.A. Stefaniak, F. Pointurier, O. Marie, J. Truyens, Y. Aregbe, Analyst 139 (2014) 668-675.

[18] T. Yomogida, F. Esaka, M. Magara, Anal. Methods 9 (2017) 6261-6266.

[19] G. Tamborini, D. Phinney, O. Bildstein, M. Betti, Anal. Chem. 74 (2002) 6098-6101.

[20] V. Stebelkov, I. Elyantyev, M. Hedberg, M. Wallenius, A.L. Fauré, J. Radioanal. Nucl. Chem. 315 (2018) 417-423.

[21] E.A. Stefaniak, A. Alsecz, I.E. Sajo, A. Worobiec, Z. Mathé, S. Török, R. Van Grieken, J. Nucl. Mat. 381 (2008) 278-283.

[22] E.A. Stefaniak, L. Darchuk, D. Sapundjier, R. Kips, Y. Aregbe, R. Van Grieken, J. Molec. Struct. 47 (2013) 206-212.

[23] E. Villa-Aleman, M.S. Wellons, J. Raman Spectrosc. 47 (2016) 865-870.

[24] G.C. Allen, I.S. Butler, T. Nguyen Anh, J. Nucl. Mat. 144 (1987) 17-19.

[25] P.R. Graves, Appl. Spectrosc. 44 (1990) 1665-1667.

[26] M.L. Palacios, S.H. Taylor, Appl. Spectrosc. 54 (2000) 1372-1378.

[27] M. Amme, B. Renker, B. Schmid, M.P. Feth, H. Bertagnolli, W. Döbellin, J. Nucl. Mat. 306 (2002) 202-212.

[28] D. Manara, B. Renker, J. Nucl. Mat. 321 (2003) 233-237.

[29] S. Bastians, G. Crump, W.P. Griffith, R. Withnall, J. Raman Spectrosc. 35 (2004) 726-731.

[30] S.D. Senanayake, R. Rousseau, D. Colegrave, H. Idriss, J. Nucl. Mat. 342 (2005) 179-187.

[31] M. Mellini, F. Riccobono, Chemosphere 60 (2005) 1246-1252.

[32] D.F. Roeper, D. Chidambaram, G.P. Halada, C.R. Clayton, Electrochim. Acta 51 (2006) 4815-4820.

[33] R.L. Frost, J. Čejka, M.L. Weier, J. Raman Spectrosc. 38 (2007) 1609-1614.

[34] H. He, Z. Ding, D.W. Shoesmith, Electrochem. Com. 11 (2009) 1724-1727.

[35] C. Jégou, R. Caraballo, S. Peuget, D. Roudil, L. Desgranges, M. Magnin, J. Nucl. Mat. 405 (2010) 235-243.

[36] H. Idriss, Surface Science Reports, 65 (2010) 67-109.

[37] A. Canizarès, G. Guimbretière, Y.A. Tobon, N. Raimboux, R. Omnée, P. Perdicakis, B. Muzeau, E. Leoni, M.S. Alam, E. Mendes, D. Simon, G. Matzen, C. Corbel, M.F. Barthe, P. Simon, J. Raman Spectrosc. 43 (2012) 1492-1497.

[38] L. Desgranges, G. Baldinozzi, P. Simon, G. Guimbretière, A. Canizares, J. Raman Spectrosc. 43 (2012) 455-458.

[39] J. Plaue, Forensic signatures of chemical process history in uranium oxides (2013), UNLV Thesis/Dissertations/Professional papers/Capstones, Paper 1873, University of Las Vegas, Nevada, USA.

[40] G. Guimbretière, L. Desgranges, C. Jégou, A. Canizares, P. Simon, R. Carabello, N. Raimboux, M.F. Barthe, M.R. Ammar, O.A. Maslova, F. Duval, R. Omnée, IEEE Trans. Nucl. Sci. 61 (2014) 2045-2051.

[41] R.M. Bell, M.A. Jeppesen, J. Chem. Phys. 3 (1935) 245-247.

[42] R.J. Gillespie, E.A. Robinson, Canadian J. Chem. 40 (1962) 644-657.

[43] I.A. Degen, G.A. Newman, Spectrochim. Acta 49A (1993) 859-887.

[44] L. Burgio, R.J.H. Clark, Spectrochim. Acta A 57 (2001) 1491-1521.

[45] R.L. Frost, J. Čejka, M.L. Weier, J. Raman Spectrosc. 38 (2007) 460-466.

[46] L.E. Sweet, T.A. Blake, C.H. Henager Jr, S. Hu, T.J. Johnson, D.E. Meier, S.M. Peper, J.M. Schwantes, J. Radioanal. Nucl. Chem. 296 (2013) 105-110.

[47] V.A. Volkovich, T.R. Griffiths, D.J. Fray, M. Fields, Vib. Spectrosc. 17 (1998) 83-91.

[48] S. Manna, S.B. Roy, J.B. Joshi, J. Nucl. Mat., 424 (2012) 94-100.

[49] R. Eloirdi, D. Ho Mer Lin, K. Mayer, R. Caciuffo, T. Fanghänel, J. Mater. Sci. 49 (2014) 8436-8443.

[50] N. Raje, S. Manna, D.K. Ghonge, A.V.R. Reddy, J. Anal. Applied Pyrolysis 109 (2014) 21-28.

Captions of figures

Table 1. Processing history of samples

Fig. 1. Average Raman BA spectrum (B, black curve) and average Raman SPA spectra (P1, P2, and P3, blue, red and purple curves, respectively) for the El Mesquite UOC (UP). All spectra are normalized with respect to the most intense band.

Fig. 2. Average Raman BA spectrum (B, black curve) and average Raman SPA spectrum (P, blue curve) for the Ranstad UOC (SDU). All spectra are normalized with respect to the most intense band.

Fig. 3. Average Raman BA spectrum (B, black curve) and average Raman SPA spectrum (P, blue curve) for the Denison UOC (ADU). All spectra are normalized with respect to the most intense band.

Fig. 4. Average Raman BA spectrum (B, black curve) and average Raman SPA spectra (P1, P2, and P3, blue, red and purple curves, respectively) for the Olympic Dam UOC (TUO). All spectra are normalized with respect to the most intense band in the 200—600 cm^{-1} region.

Fig. 5. Average Raman BA spectrum (B, black curve) and average Raman SPA spectra (P, blue curve) for the Susquehanna UOC. All spectra are normalized with respect to the most intense band.

Fig. 6. Average Raman SPA spectra the Ranstad (R, gray), Denison (D, black), Olympic Dam (O, blue) and Susquehanna (S, purple) UOCs in the 900—1200 cm^{-1} region. All spectra are normalized with respect to the most intense band in this region. No bands in this region were detected for El Mesquite UOC.

Table 1. Processing history of samples

Sample, chemical formula and U-ore mine	***Information***
Uranyl peroxide (UP), $UO_4{\cdot}4(H_2O)$, El Mesquite mine	USA Texas Mobil; sandstone-roll front, low temperature redox, $NaHCO_3$ leach, precipitation with H_2O_2.
Sodium di-uranate (SDU), $Na_2U_2O_7$, Ranstad mine	Sweden; black shale, low temperature redox, strong H_2SO_4 leach with no oxidiser, solvent exchange with tertiary amine, $Na_2CO_3/(NH_4)_2CO_3$ strip, precipitation with NaOH.
Ammonium di-uranate (ADU), $(NH_4)_2U_2O_7$, Denison mine	Canada; quartz-pebble conglomerate, non-redox, H_2SO_4 leach with $NaClO_3$ as oxidant, Strong base ion exchange with HNO_3 as eluent, Impurity precipitation with CaO and NH_3, precipitation with NH_3.
Tri-uranium octo-oxide (TUO), U_3O_8, Olympic Dam mine	Australia; Hematite breccia complex, high temperature redox, solvent exchange with Alamine 336, $(NH_4)_2SO_4/NH_3$ strip, precipitation with NH_3 and calcination to form oxide.
Uranyl hydroxide (UH), $UO_2(OH)_2$, Susquehanna mine	USA; sandstone, low temperature redox, acid leach and solvent exchange. Limited information available for this UOC as sample can come from three different sites (South Dakota, Three Rivers, Falls City).

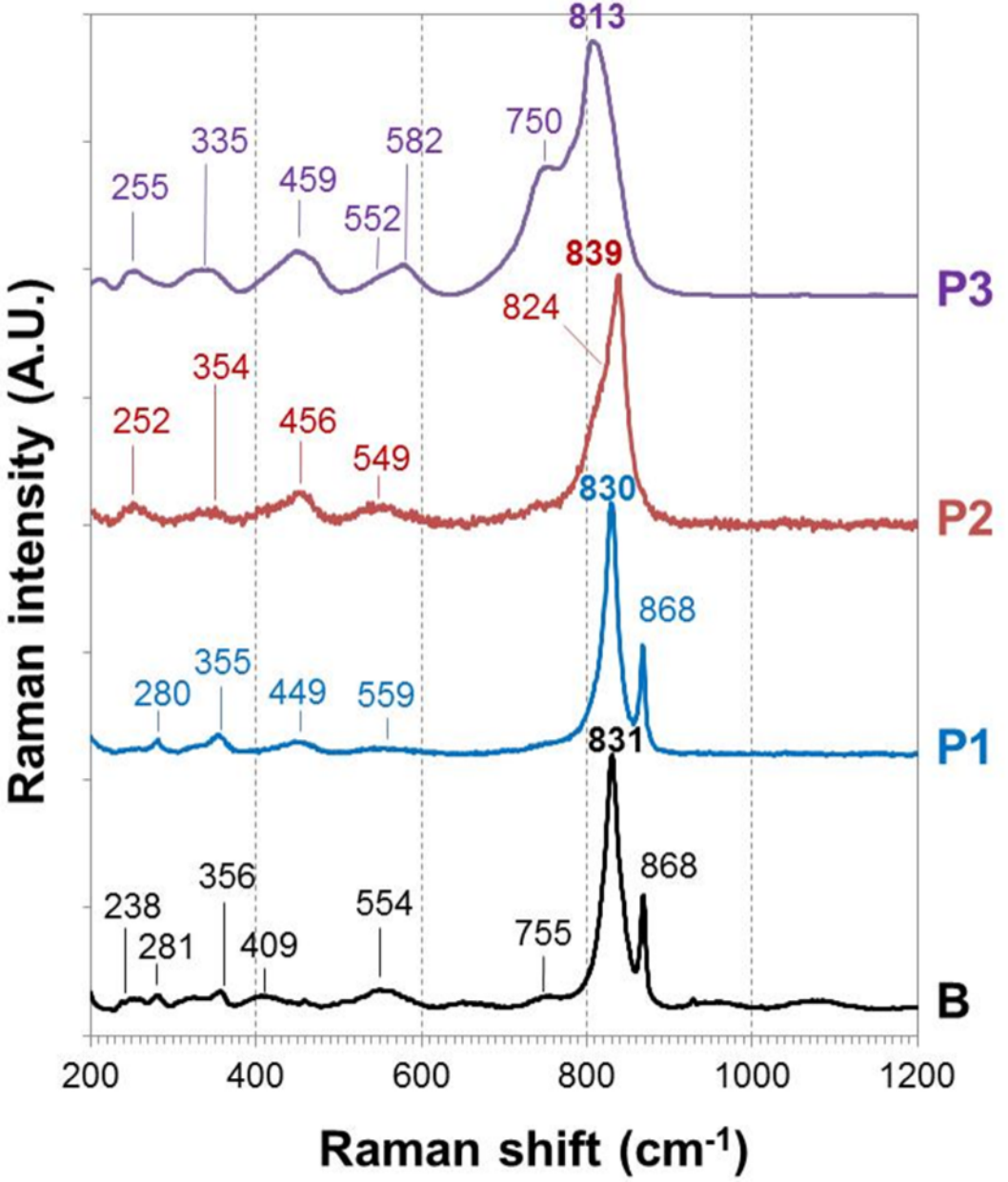
813
335
750
582
255
459
552
839
824
P3
354
252
456
549
830
P2
868
355
280
449
559
831
P1
356
868
238
554
281
409
755
B
Raman intensity (A.U.)
200
400
600
800
1000
1200
Raman shift (cm-1)

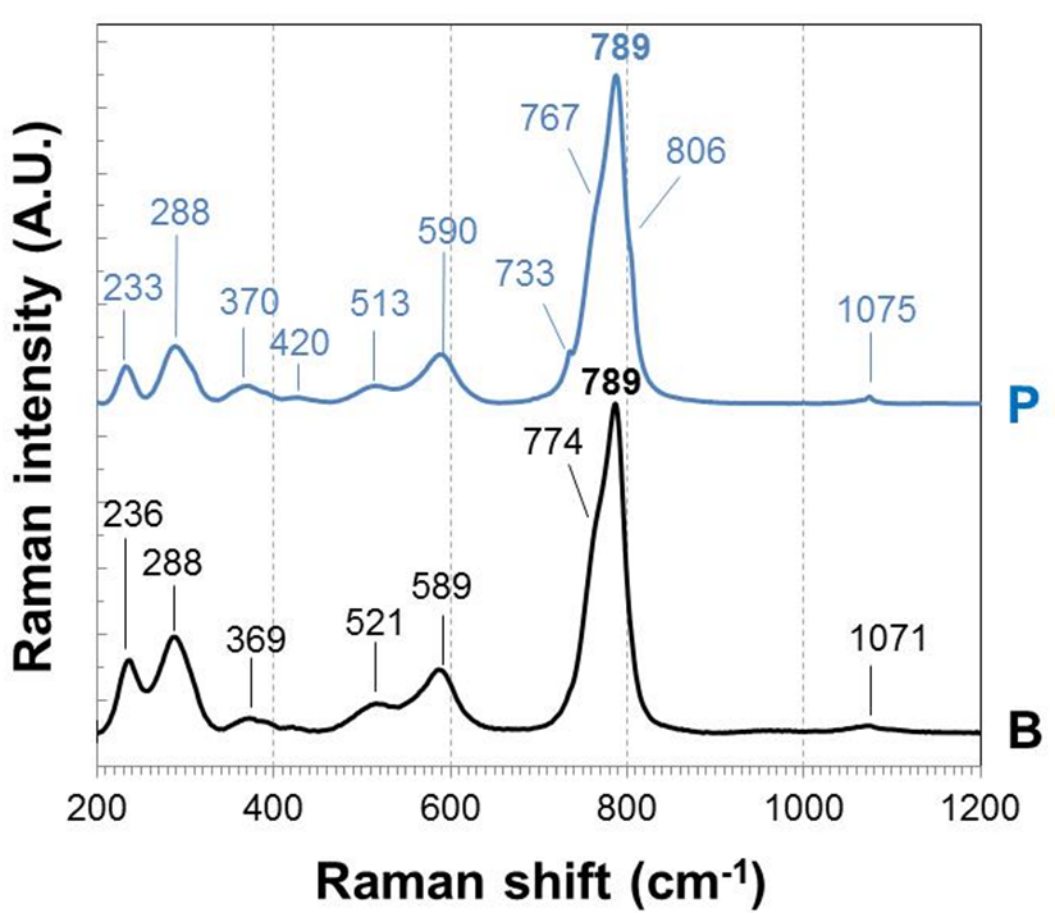
789
767
806
288
590
733
233
370
513
420
1075
P
789
774
236
288
589
369
521
1071
B
Raman intensity (A.U.)
200
400
600
800
1000
1200
Raman shift (cm-1)

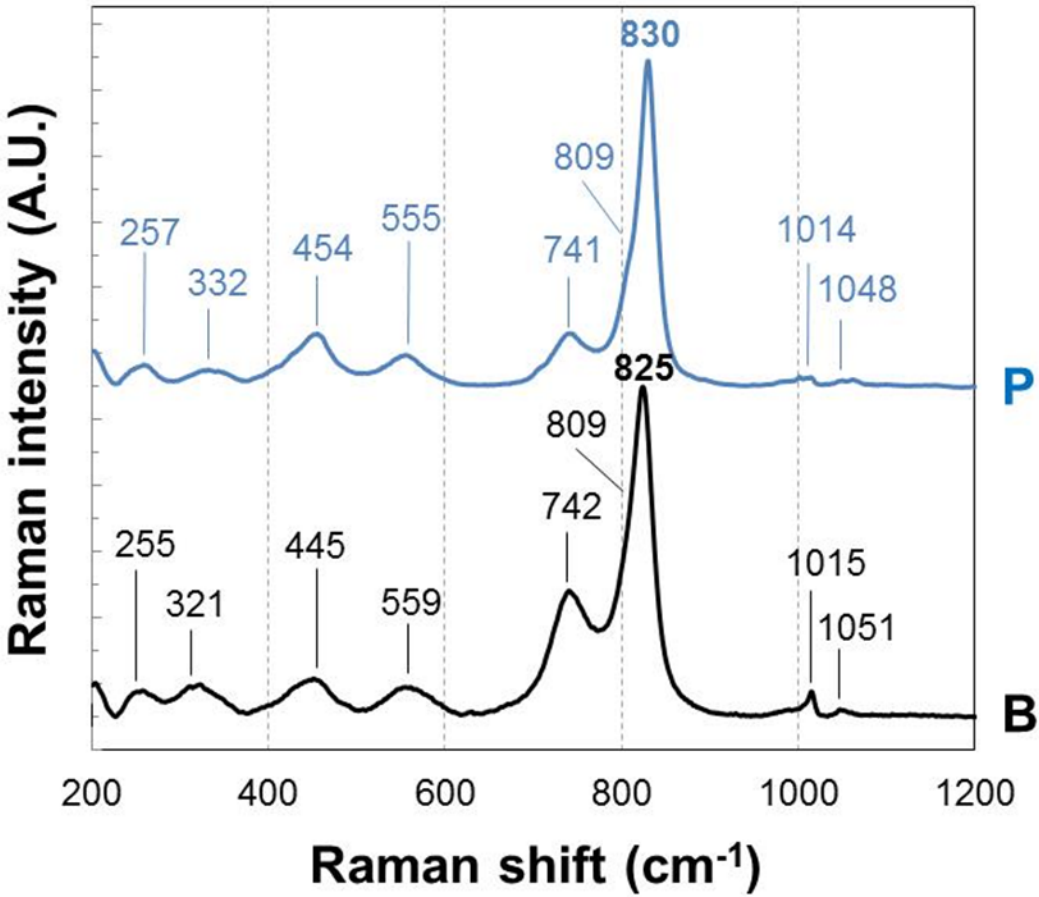
Raman intensity (A.U.)
830
809
257
332
454
555
741
1014
1048
P
825
809
742
255
321
445
559
1015
1051
B
200
400
600
800
1000
1200
Raman shift (cm-1)

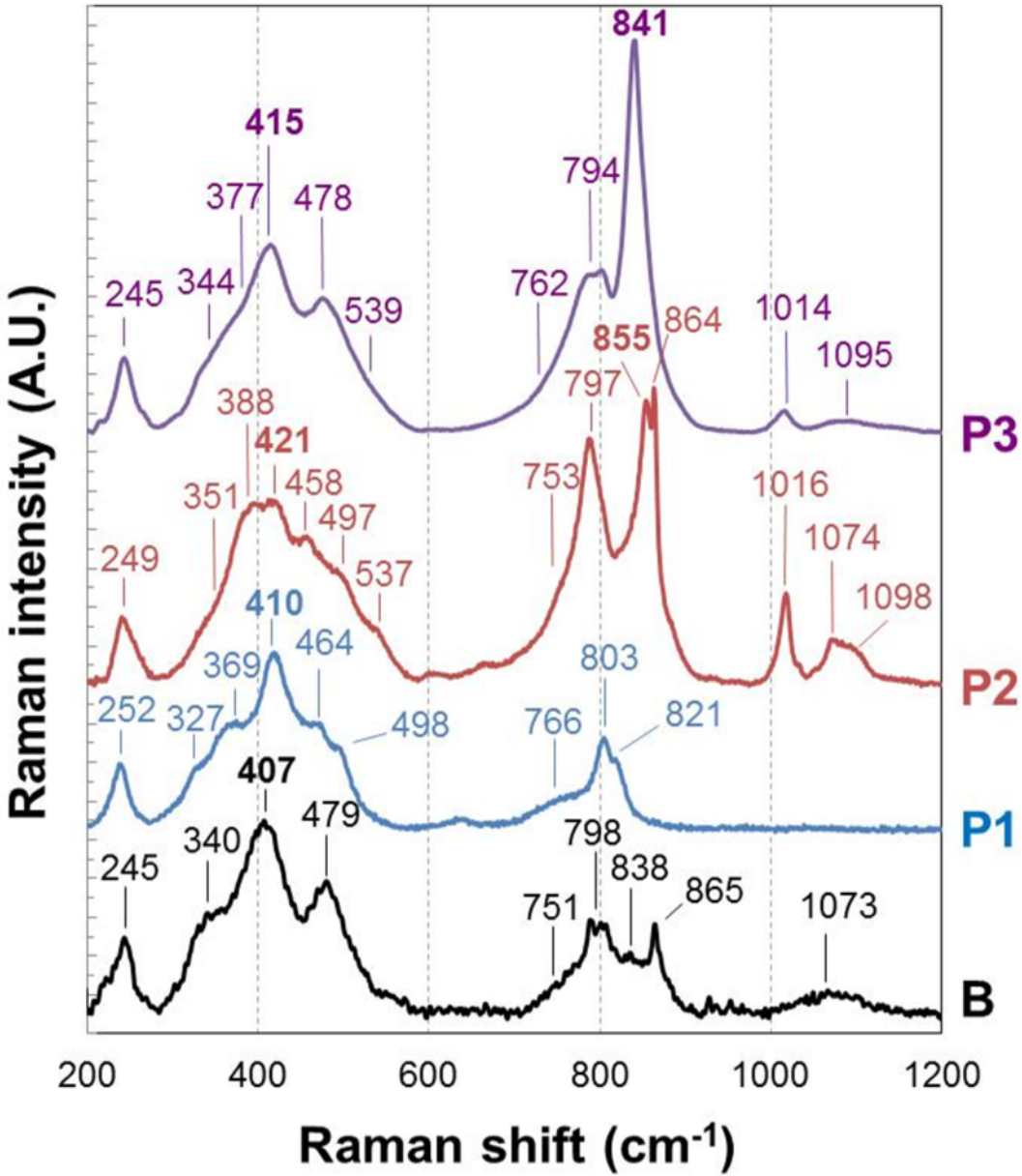
Raman intensity (A.U.)
Raman shift (cm-1)
200
400
600
800
1000
1200
P3
841
415
794
377
478
245
344
762
539
1014
855
864
1095
797
P2
388
421
753
351
458
1016
497
1074
249
537
1098
410
464
803
369
P1
252
327
498
766
821
407
479
798
340
838
245
751
865
1073
B

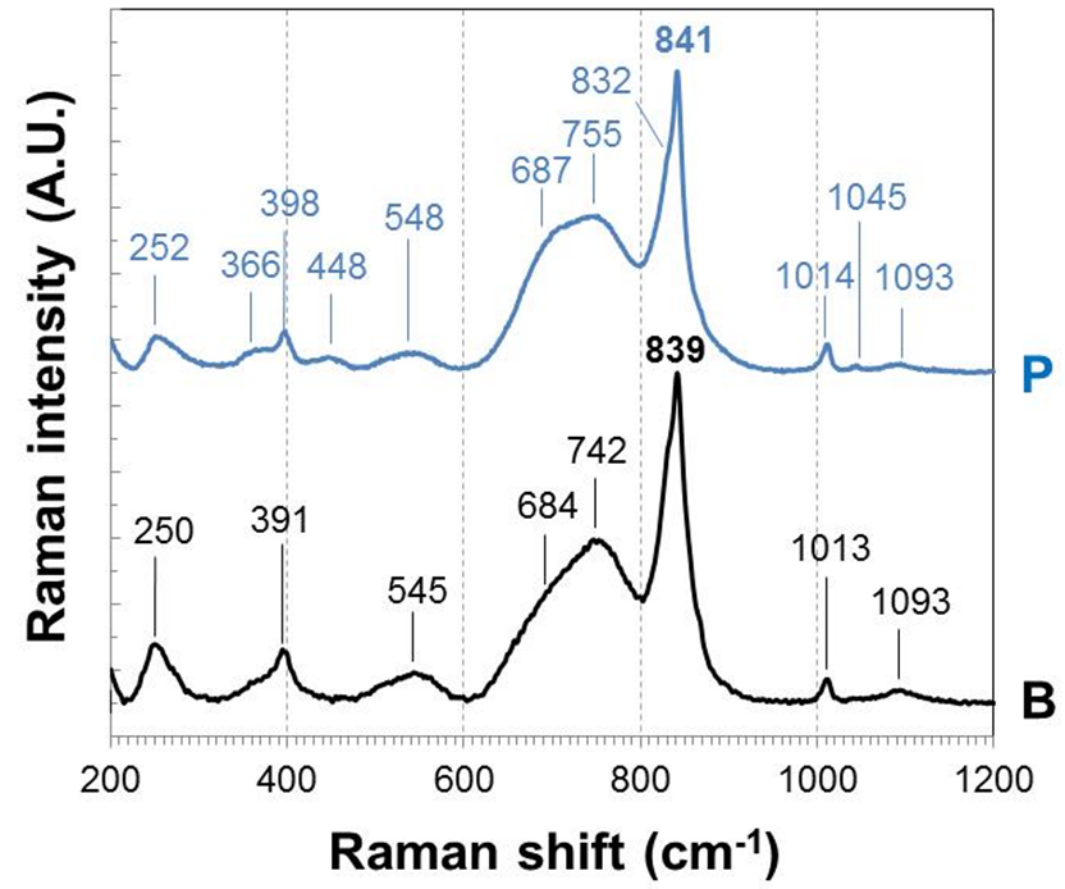
Raman intensity (A.U.)
841
832
755
687
398
548
252
366
448
1045
1014
1093
P
839
742
684
250
391
545
1013
1093
B
200
400
600
800
1000
1200
Raman shift (cm-1)

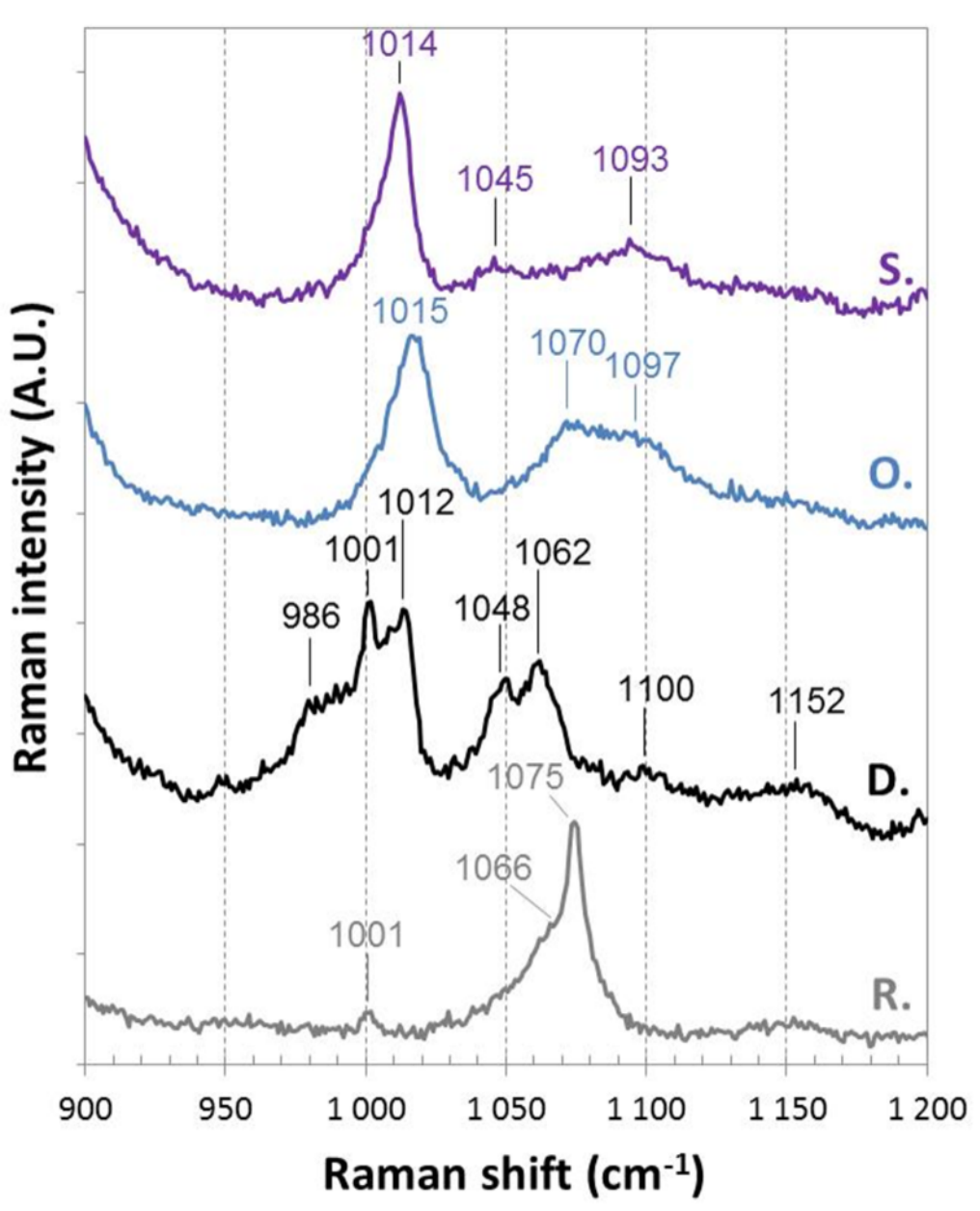
1014
1045
1093
S.
1015
1070
1097
O.
1012
1001
1062
986
1048
1100
1152
D.
1075
1066
1001
R.
Raman intensity (A.U.)
900
950
1 000
1 050
1 100
1 150
1 200
Raman shift (cm-1)